Stability and Structures of Liquid Crystalline Phases Formed by Branched-Chain Phospholipid Diastereomers

Frank Bringezu,*,† Gert Rapp,‡ Bodo Dobner,§ Peter Nuhn,§ and Gerald Brezesinski‡

Department of Chemical Engineering, Eng. II, University of California, Santa Barbara California 93106-5080, Max Planck Institute of Colloids and Interfaces, Am Muehlenberg 1, D-14476 Golm/Potsdam, Germany, and Institute of Pharmaceutical Chemistry, Martin-Luther-University Halle, D-06099 Halle, Germany

Received: November 22, 2000

Diastereomers of 1-alkyl-2-acylglycerophosphocholines containing 2-methyl-branched fatty acids at the C2 position of the glycerol are synthesized and separated, varying the acyl-chain systematically ($m = 13$, 15, 17). The physicochemical properties are studied in monolayers at the air−water interface by pressure area isotherms and grazing incidence X-ray diffraction (GIXD) measurements. The phase behavior is examined by a combination of differential scanning calorimetry and time-resolved X-ray diffraction experiments. In monolayers at the air−water interface, the introduction of a methyl-branch disturbs the lateral packing drastically, resulting in phases with strongly tilted chains and an undefined tilt azimuth. The monolayer structures of the diastereomeric fractions cannot be distinguished. The comparison of the lyotropic mesophases of the aqueous dispersions shows comparable structural parameters. The temperature dependency of the *d* spacings is nonlinear and is discussed in terms of a critical swelling of the bilayer. The present experiments show that the two racemic pairs of the resolved diastereomers (*SS* + *RR*/*SR* + *RS*) exhibit pronounced differences in the thermodynamic parameters of phase transitions both in two-dimensional (monolayers at the air/water interface) and three-dimensional systems (aqueous dispersions). However, the influence of the chiral carbon atoms is not sufficient to change the structure of the phases despite being able to affect their stability.

Introduction

Biological membranes are complex mixtures of lipids and proteins. The typical bilayer structure is determined by membrane lipids forming a liquid-crystalline matrix under physiological conditions. One approach to the question of how lipid species change the structure and thermodynamic parameters in bilayers are experiments with lipid−water model systems. Therefore, the phase behavior of aqueous lipid dispersions and two-dimensional model systems (monolayers) of membrane lipids, particularly phosphatidylcholines (PCs) and phosphatidylethanolamines (PEs), which are known to be the major components of biological membranes, has been studied by an enormous number of physicochemical techniques.[1−3]

In biological membranes, the fluidity can be adapted to environmental conditions by regulation of the phospholipid/cholesterol ratio or by changing the fatty acid composition of phospholipids by the introduction of either unsaturated chains or branches in the hydrophobic part of the lipid molecules. Despite the important role of branched chain lipids, very little is known about their physicochemical properties.[4−6] Branched-chain lipids are interesting model systems for these studies not only because they are found in biological systems,[7] but moreover, because they enable investigations of general features determining the structure of mono- and bilayers.[8−11] The variation of position and length of the branches in the hydrophobic region of the molecules allows systematic changes in the relative size of the hydrophilic and hydrophobic parts. The influence of the structure of both the hydrophobic and hydrophilic (headgroups) regions on the ordering in two- and three-dimensional systems has been extensively studied.[12−14] In bulk systems, the introduction and stepwise elongation of side-chains shift the main-transition (gel to liquid crystalline) temperature T_m of aqueous dispersions first to lower values and then, after reaching a minimum, the T_m values start to increase. This systematic change in T_m is connected with a modified structural polymorphism.[6] Within homogeneous phases, the temperature dependence of the *d* values is mostly linear. However, several investigations[15−17] have revealed a nonlinear increase of the *d* values approaching the phase transition temperature on cooling. Such a behavior is described as a critical swelling of bilayers.[18,19]

In monolayers at the air−water interface, the competitive interactions between hydrophobic and hydrophilic parts of the molecules determine the structure of a condensed film. It has been shown that the chains of DPPC are strongly tilted due to the large headgroup size even at the highest lateral pressure.[20] The introduction of side groups in the hydrophobic region of phospholipids drastically changes the molecular packing. In the case of PCs substituted with long-chain alkyl branches in the 2-position of the fatty acids, GIXD measurements have shown that the packing of the molecules is now determined by the space requirements of the chains rather than that of the headgroup.[20] Nevertheless, the comparison of the pure enantiomers and the racemate of such a triple-chain PC revealed differences in the monolayer structure at least at low lateral pressures.[9]

Despite the importance of chirality in the structure formation of biological materials, less is known about the influence of stereochemical variations on the phase behavior of phospho-

* To whom correspondence should be addressed.
† University of California, Santa Barbara.
‡ Max Planck Institute of Colloids and Interfaces.
§ Martin-Luther-University Halle.

10.1021/jp0042720 CCC: $20.00
Published on Web 02/07/2001

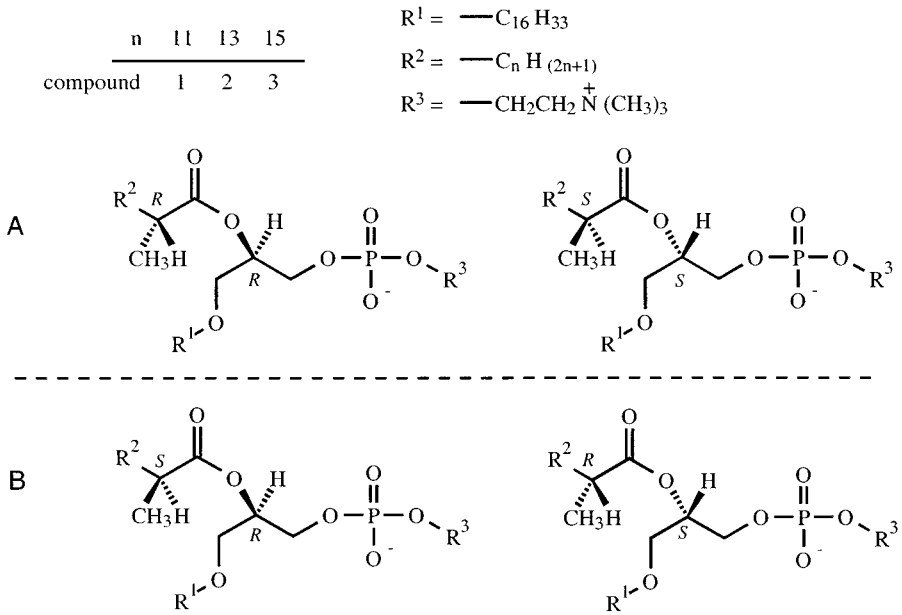

Figure 1. Enantiomers of the phosphatidylcholines (R^3) synthesized contain at the C1 position of the glycerol backbone a C16 hydrocarbon chain (R^1) attached via an ether linkage. The length of the methyl-branched chain (R^2) at the C2 position of the glycerol has been varied ($n = 11, 13, 15$). Part A shows the first eluting fraction of diastereomers and part B the second fraction. The configuration at the chiral carbon atoms is marked.

TABLE 1. Analytical Characterization of the 1-*O*-Hexadecyl-2-acyl-GPCs (1−3): The Results from the Phosphorus Analysis and the Mass Spectrometry Are Shown[a]

	P (calcd/obsd)	yield (%)	mol wt calcd/mol peak MS	t_{Ra} (s)	t_{Rb} (s)	A_a (%)	A_b (%)	α
1	4.35/4.48	75	692.0/692.7 $(M + H)^+$	21.5	24.1	98.2	98.5	1.12
2	4.23/4.30	73	720.1/720.7 $(M + H)^+$	21.0	23.8	98.3	98.6	1.13
3	4.15/4.14	70	748.1/748.7 $(M + H)^+$	23.3	26.0	99.8	99.4	1.12

[a] The retention times of the diastereomers (t_{Rb}, t_{Ra}), the integrated areas (A_a, A_b) of the preparative isolated diastereomers, and the resulting separation coefficients (α) obtained in HPLC measurements are given.

lipids. Lipid dispersions as well as lipid monolayers are suitable model systems to study the relationship between chirality and structure. The introduction of short-chain branches in the 2-position of the acyl chain leads to a second chiral center; hence, these compounds consist of diastereomers. In the case of 1-alkyl-2-(2′-methylacyl)glycerophosphocholines, these diastereomers were quantitatively resolved and the absolute configuration of the products determined.[21,22] These studies have shown that the separation of the diastereomeric fractions drastically depends on the distance between the two chiral carbon atoms. In the case of a 2-methyl-branching, a quantitative separation was possible, whereas for the 3-methyl-branched derivative only HPLC analysis could provide a distinction between the fractions. Further increasing the distance between the chiral atoms suppresses the separation completely. The possibility of separating the diastereomers quantitatively by column chromatography already indicates differences in the physicochemical parameters. Therefore, different phase transition parameters of the biomimetic lipid−water systems must be expected and influences of stereochemistry on the supramolecular structures cannot be excluded.

The present work reports the first results on the phase behavior of isolated diastereomers of racemic 1-alkyl-2-acylglycerophosphocholines containing a 2-methyl-branched acyl chain. Calorimetric and X-ray diffraction experiments were used for the characterization of aqueous dispersions in the water-saturated two-phase region. Grazing incidence X-ray diffraction (GIXD) and pressure/area isotherm measurements provide information about the phase behavior of monolayers at the air/water interface.

Experimental Section

Synthesis. The branched-chain fatty acids were prepared by alkylation of methyl malonic acid esters with long-chain alkylhalogenides.[23] The structure of the fatty acids was confirmed by mass spectrometry. The purity of the products was checked using gas chromatography of the methyl esters. The melting points of the fatty acids were found to be in agreement with the literature data.[23,24] Epichlorhydrine used as starting material was transformed in several steps to the racemic 1-*O*-hexadecylglycero-3-phosphocholine, which was then acylated with branched chain fatty acid anhydrides in the presence of 4,4′-(dimethylamino)pyridine to the corresponding 1-*O*-hexadecyl-2-acylglycero-3-phosphocholines.[13,25] The purification was carried out using column chromatography. The column was packed with 100 g of silica gel per gram of the crude product. A gradient elution using 100 mL chloroform, followed by 100 mL of chloroform/methanol/25% ammonia solution (90/10/1 v/v), 100 mL (80/20/2), 100 mL (70/30/3), and 100−400 mL (65/35/5) yields two pairs of diastereomers of the branched-chain glycerophosphocholines **1**−**3** (see Figure 1). For nomenclature, we applied the letter **a** to the first eluting fraction and the letter **b** to the second fraction throughout this paper. The characterization of the compounds was carried out using HPLC, FAB (fast atom bombardment) mass spectroscopy, microanalysis, and ^{1}H NMR (see Table 1 and ref 21). The ^{1}H NMR spectra of the isolated fractions (**1**−**3a**,**b**) were measured to confirm the absence of 1,3-isomers, which would show differences in the chemical shift of the proton at the C2 position of the glycerol. However, for this proton in all cases a multiplett at 5.07−5.09 ppm was obtained. Further detailed analysis by ^{1}H-COSY

spectra and comparison with literature data[26] allowed the assignment of the ^{1}H signals, excluding the presence of 1,3 isomers.

Physicochemical Characterization. Differential scanning calorimetry (DSC) has been used for the characterization of the thermotropic phase behavior of the lipid-water dispersions in the water-saturated two-phase region (60 wt %) using a Perkin-Elmer (Norwalk, CT) DSC-2 instrument. Initially, all lipids were dried in a vacuum oven for 2 h at 50 °C before weighing. The 3−5 mg samples were transferred into aluminum pans and mixed with water before sealing. Multilamellar dispersions were formed by equilibration above the main-transition temperature (T_m) for 1 h. An empty pan was used as a reference. The data were recorded through an interface to a PC. After a polynomial baseline fit, the transition enthalpies and main-transition temperatures have been determined. The amount of strongly bound water was quantitatively calculated from the ice peak resulting from the melting of frozen excess water not bound to the headgroups.[27]

The monolayer experiments have been performed using a home-built trough equipped with a Wilhelmy-type pressure-measuring device. The pure lipids were dissolved in chloroform adding small amounts of methanol and then spread onto pure water (Millipore Milli-Q, 18 MΩcm).

Grazing incidence X-ray diffraction (GIXD) measurements were performed at 15 °C using the liquid surface diffractometer on the beam line BW1 at HASYLAB, DESY, Hamburg, Germany. The synchrotron beam was made monochromatic by a Beryllium (002) crystal. Experiments were performed at an angle of incidence of $0.85\alpha_c$ (α_c is the critical angle for total external reflection). A linear position sensitive detector (PSD) (OED-100-M, Braun, Garching, Germany) was used for recording the diffracted intensity as a function of both the vertical (Q_z) and the horizontal (Q_{xy}) scattering vector components. The analysis of the in-plane diffraction data yields lattice spacings according to $d_{hk} = 2\pi/Q_{xy}^{hk}$. From the maximum of the Bragg rods it is possible to derive information about the tilt angle and direction of tilt due to $Q_z^{hk} = Q_{xy}^{hk} \tan(t)\cos(\psi_{hk}^*)$. For further details about GIXD the reader is referred to the literature.[28−30]

Time-resolved X-ray measurements were carried out at the ×13 double focusing monochromator-mirror camera[31] of the EMBL outstation at DESY, Hamburg, Germany, by using a monochromatic X-ray beam ($\lambda = 0.15$ nm). The diffracted intensities in the small- and wide-angle regions were simultaneously recorded using a data acquisition system described elsewhere.[32] The diffraction patterns were registered during the heating−cooling cycles at a scan rate of 1 °C/min^{-1}. The reciprocal spacings $s = 1/d$ were calibrated by the diffraction pattern of dry rat-tail collagen with a long spacing of 65 nm (SAXS) and *p*-bromobenzoic acid (WAXS). For sample preparation, weighted amounts of the lipid were dispersed in pure water (60 wt %). The dispersions were vortexed and then transferred into glass capillaries (diameter = 1 mm) (Hilgenberg, Malsfield, Germany), which were placed in the temperature controlled sample holder.

Results

All diastereomers isolated form stable monolayers at the air/water interface. Figure 2 displays the isotherms obtained for compounds **3a** and **3b** at 15 °C. The isotherm of **3a** is fully condensed. In the case of **3b**, the pressure offset begins at about 104 Å^2/molecule. At 6 mN/m the isotherm shows an inflection point followed by a plateau region indicating a first-order transition from a liquid-expanded (l.e.) to a liquid-condensed (l.c.) phase. The transition enthalpy ΔH calculated from the area change involved in the transition amounts to ∼50 kJ/mol. Obviously the monolayers of **3a** and **3b** show differences in the thermodynamic parameters of the phase transition. Compounds **1a** and **1b** display only an l.e. phase in the whole pressure region up to 40 mN/m. Compounds **2a** and **2b**, with the medium acyl chain length, exhibit a smeared-out plateau region with a higher transition pressure for compound **2b**.

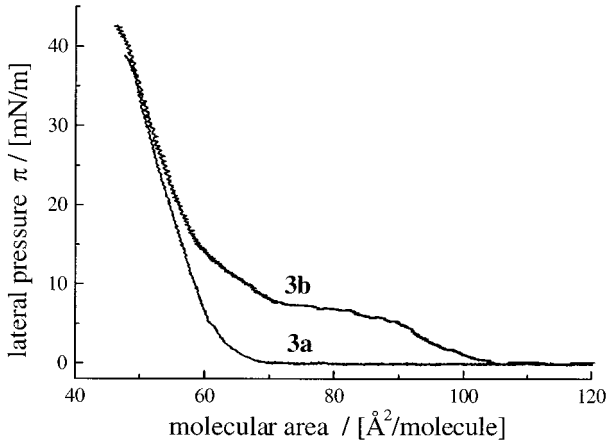

Figure 2. Pressure area isotherms of the diastereomers **3a** and **3b** at 15 °C.

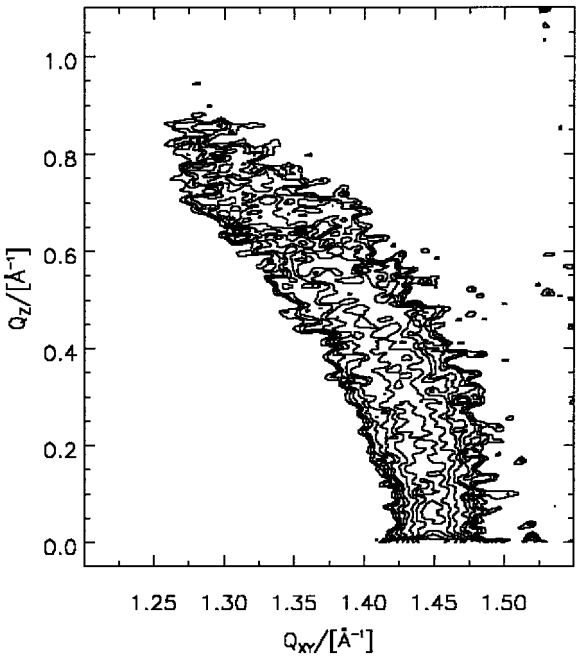

Figure 3. Contour plot of the corrected X-ray intensities as a function of the in-plane component Q_{xy} and the out-of-plane component Q_z of the scattering vector **Q** for the diastereomer **3a** at 15 °C and 35 mN/m.

GIXD studies should provide information about the structure of the condensed monolayer phases. Our investigations are focused on compounds **3a** and **3b**, which have the largest pressure region for condensed phases. At lower pressures, the diffracted intensity is very low for both compounds. Figure 3 shows the contour plot of the corrected X-ray diffraction intensities as a function of the in-plane (Q_{xy}) and the out-of-plane scattering vector components (Q_z) for **3a** at 15 °C and 35 mN/m. Compound **3b** exhibits an identical contour plot, hence possible structural differences of the condensed phases of these two compounds cannot be resolved.

DSC thermograms of the lipid-water dispersions, taken at a scan rate of 1.25 °C/min after equilibration above the main

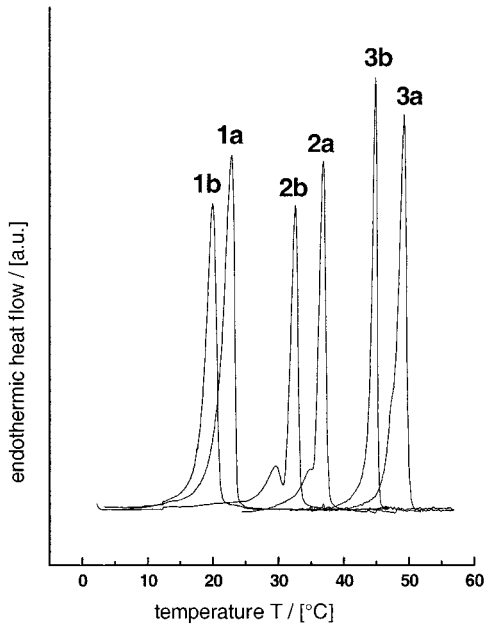

Figure 4. Comparison of DSC thermograms of aqueous (water-saturated two-phase region) dispersions of compounds **1**−**3** taken at a scan rate of 5 K/min after homogenization above the main transition temperatures.

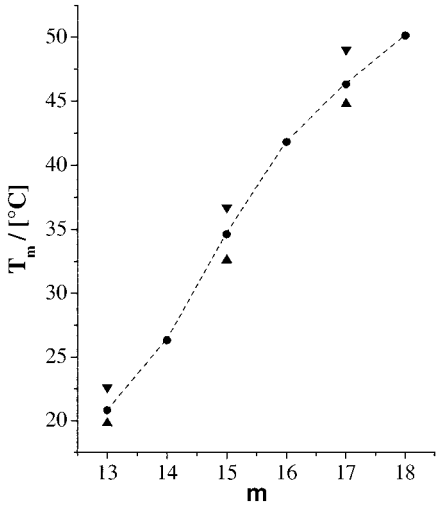

Figure 5. Main-transition temperatures T_m of 1-hexadecyl-2-(2-methylacyl)glycerophosphocholine−water dispersions as a function of the length m of the methyl-branched acyl chain. ▼ = first eluting fraction of diastereomers, ▲ = second eluting fraction of diastereomers, ● = 1:1 mixture of diastereomers. The data for m = 14, 16, and 18 have been published previously (see ref 13).

transition, are shown in Figure 4. All diastereomers isolated show a main-transition from a gel to a liquid-crystalline phase. The corresponding pairs of diastereomers show differences in the main-transition temperatures (T_m). In all cases, the diastereomers exhibiting the smaller retention time in the HPLC measurements (**1a**, **2a,** and **3a**) display the higher T_m values (Figure 5). The transition enthalpies calculated from the peak areas also show differences (for details see Table 2) except for compounds **3a** and **3b**. Comparing heating and cooling scans, all samples investigated exhibit a hysteresis of about 6 °C in the T_m values. Compounds **2a**, **2b** and **3a** exhibit in addition to the main-transition a pronounced pre-transition at 34.8, 29.5, and 47.3 °C, respectively. In the case of compounds **1a** and **b** as well as compound **3a** no pre-transition could be resolved, however, the peak shape is asymmetric. Therefore, pre-

TABLE 2. Main-Transition Temperatures (T_m), Enthalpies (ΔH), and Amount of Water Bound to the Head Group Obtained from DSC Measurements of the 1-*O*-Hexadecyl-2-acyl-GPCs 1−3 in the Water-Saturated Two-Phase Region (60 wt % Water)

lipid	T_m (°C)	ΔH (kJ/mol)	bound water (mol W/mol L)
1a	22.6	27.6	11.5
1b	19.8	26.4	9.5
2a	36.7	33.9	12.4
2b	32.6	33.2	13.4
3a	49.0	40.6	10.2
3b	44.8	40.3	9.7

transitions cannot be excluded. All lipid-water dispersions have been investigated up to 97 °C and no further transitions have been observed. Comparing the T_m values of compounds **1** to **3** with those found for the corresponding mixtures of diastereomers with an even number m ($m = n + 2$) of carbon atoms in the acyl chain (see ref 13), a continuous increase of T_m with increasing acyl chain length is observed (see Figure 5). From freezing and melting the samples, the amount of water bound to the headgroups was calculated. The results show that for compounds **1a** and **1b** (shortest acyl chain) the diastereomers display pronounced differences. As the acyl-chain length increases from compound **1**−**3**, these differences vanish (see Table 2).

Both the high transition enthalpy and the hysteresis obtained in DSC measurements indicate, that a typical main-transition from a gel to a liquid-crystalline phase must be assumed for the second and further heating runs. First X-ray exposures of the 60 wt % water dispersion of compound **1a** taken after a prolonged storage at 4 °C show two reflections in the SAXS (0.21 nm^{-1}, 0.42 nm^{-1}) and multiple reflections in the WAXS indicating a lamellar structure of phospholipid bilayers with crystalline chains (see Figure 6 left). On heating the sample, the multiple reflections in the WAXS disappear at 37.2 °C and a broad scattering of molten chains was obtained. Concurrently, the intensity of the sharp reflection of the L_c phase decreases and two low order reflections of a lamellar liquid-crystalline $L_{á}$-phase (Figure 6 right) appear at 0.144 nm^{-1} and 0.288 nm^{-1} corresponding to a d value of 6.94 nm. The peak widths of the first-order reflections of the L_c- and the $L_{á}$-phase are equal (0.006 nm^{-1}); however, the intensity of the second-order reflection of the $L_{á}$-phase is much larger than that of the L_c-phase. This could be an indication of good ordering within a bilayer but with comparably poor correlation between multiple layers in the case of the crystalline L_c phase. The maximum position of the halo in the WAXS at 2.2 nm^{-1} results in an area per hydrocarbon chain of 0.238 nm^2.

On cooling the sample, the maximum of the first order reflection shifts to lower s values and just before the transition into the gel phase the peak position remains constant over a small temperature range. The main-transition is indicated by a positional shift of the (10) reflection to larger s values. At 15.6 °C (Figure 7 bottom), the gel phase exhibits a long spacing of 5.61 nm, which is considerably larger than that obtained in the crystalline state. A detailed analysis of the SAXS data for sample **1a** shows that between 20.5 and 17.6 °C the typical scattering profile of a ripple phase $P_{\beta'}$ occurs (see Figure 7 middle). Therefore, the existence of a monotropic $P_{\beta'}$-phase existing between L_α and $L_{\beta'}$ must be assumed. Below the main transition the halo in the WAXS disappears and a scattering profile described as a superposition of three peaks occurs (Figure 8). The fitted peak maxima are located at 2.28, 2.35, and 2.49 nm^{-1} leading to an area per hydrocarbon chain of 0.206 nm^2. Therefore, in the gel-phase below T_m oblique chain packing must

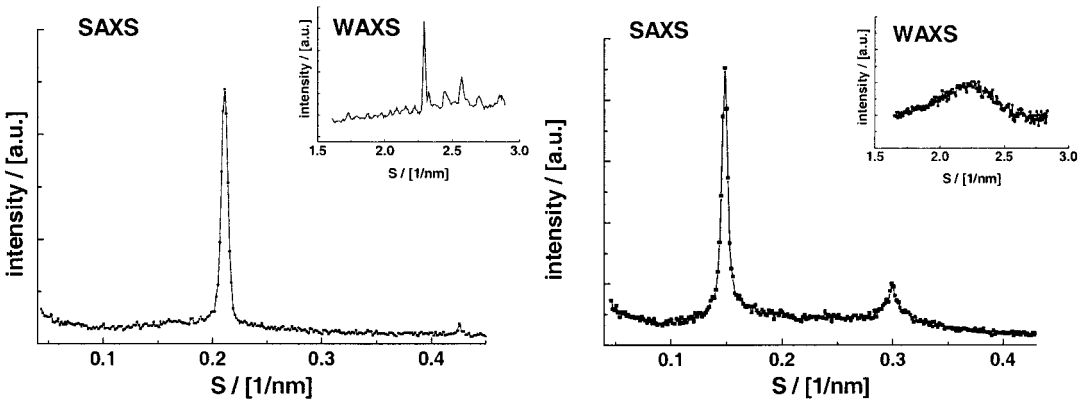

Figure 6. X-ray diffraction patterns of the SAXS and WAXS (insert) regions of aqueous dispersions of compound **1a**. Diffraction patterns at 8.5 °C (left) and 40 °C (right) taken on the first heating scan of the sample.

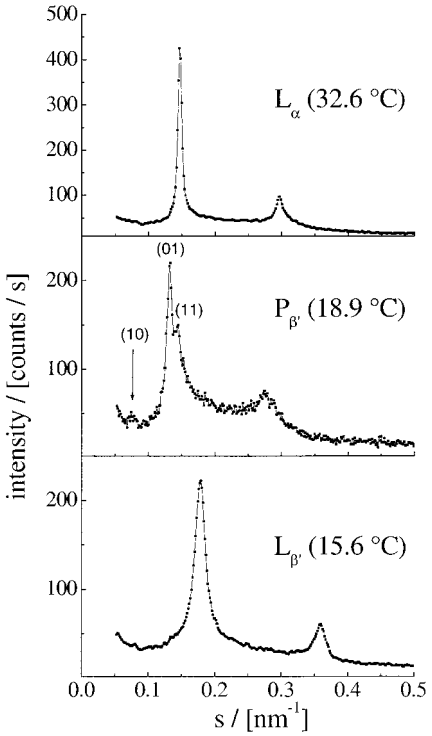

Figure 7. Small-angle X-ray diffraction patterns of aqueous dispersions (60 wt %) of compound **1a** observed on cooling with a scan rate of 0.5 °C/min.

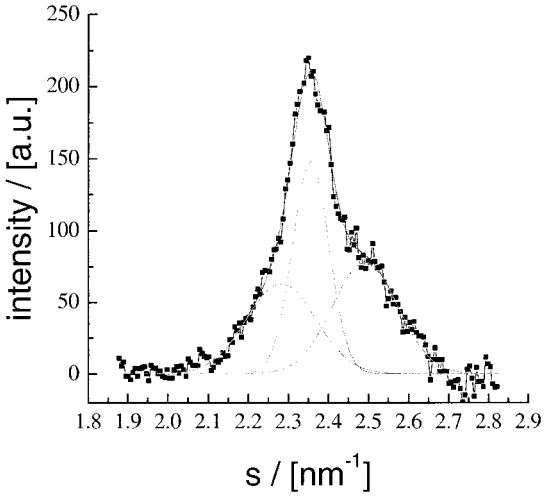

Figure 8. Wide-angle X-ray diffraction pattern of **1a** at 15.5 °C and fitted peak positions.

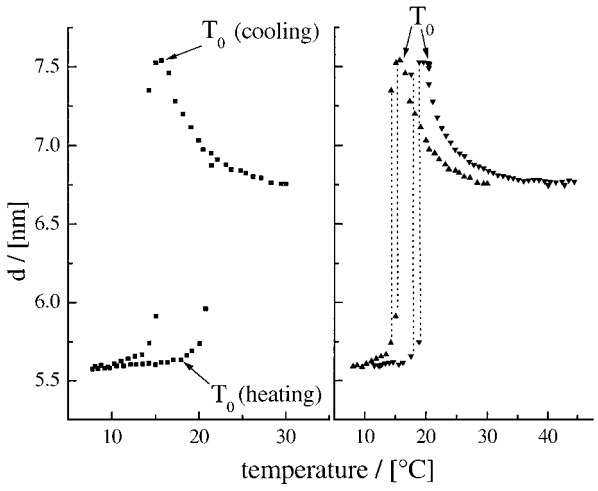

Figure 9. Temperature dependence of the lamellar *d*-spacings. The values obtained upon cyclic heating and cooling of compound **1b** at a scan rate of 1.0°C/min are shown in the left plot. The right part compares the long spacings of compounds **1a** (▼) and **1b** (▲) taken on cooling the samples. The onset temperatures (T_0) of the main transitions obtained in the DSC heating and cooling scans are marked.

be assumed. Further temperature decrease shifts the maximum positions slightly to larger values indicating a small decrease of the hydrocarbon chain area. At a temperature of 11.0 °C the values fitted amount to 2.29, 2.36, and 2.50 nm^{-1}.

Discussion and Conclusion

In the monolayer experiments, the scattered intensity is distributed over a large range of Q_{xy} and Q_z values. Such a broad scattering profile has also been obtained for methyl-branched PEs,[33] whereas the nonbranched double-chain DPPC exhibits three distinct diffraction peaks indicating an oblique lattice structure.[20] The observed distribution of the scattering intensity can be explained assuming a superposition of multiple lattices exhibiting same spacings and tilt angles, but a continuous variation in the tilt azimuth.[33,34] Therefore, the [02] reflection of a NNN (next-nearest neighbor) tilted phase can be determined from the intensity at highest Q_z (0.81 Å^{-1}) and lowest Q_{xy}. The corresponding degenerate [10],[01] reflection should have maximum intensity at 0.405 Å^{-1} which is half of the $\boldsymbol{Q}_{zmax}^{[02]}$.

The chain tilt calculated from these data amounts to (32 ± 2)° and a cross-sectional area (A_0) of 0.207 nm^2/chain can be deduced. Assuming constant tilt and A_0 values, the position of the 2-fold degenerate peak of a rectangular lattice with NN (nearest neighbor) tilt has been calculated using the position of the [02] reflection of this lattice (Q_{xy} = 1.45 Å^{-1} and zero Q_z).

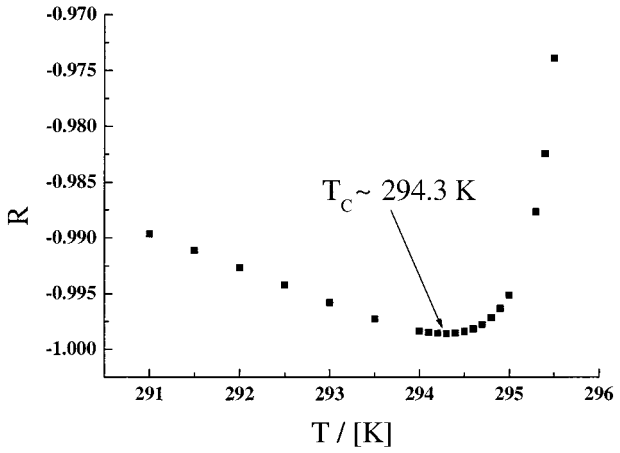

Figure 10. Correlation coefficient R of the linear fit as function of the critical temperature T_C used in the fit.

The corresponding Q_{xy} and Q_z values are 1.33 and 0.7 Å^{-1}, respectively. The remaining intensities result from oblique phases exhibiting the same tilt angle and differing only in the tilt azimuth. An alternative explanation for such an intensity distribution was given by Kjaer.[35] The extension of the Bragg rod along a curved line which follows the Scherrer ring of constant Q was explained either by mosaic spread in the normals of flat crystallites or by a bending of the crystallites. In principle, the film could be bent due to compression. But in our case, the scattered intensity does not follow the Scherrer ring and could be therefore only explained by a superposition of such curved lines.

The long spacings of the aqueous dispersion of compound **1b**, determined by small- and wide-angle X-ray scattering on heating and cooling with a scan rate of 1 °C/min, are compared in Figure 9 (left). At low temperatures, the *d* values increase slightly on heating the sample. The transition to the liquid-crystalline phase leads to a jump in the *d* values and on further increasing temperature the bilayer repeating distance decreases remarkably. At the highest temperatures investigated, a spacing of 6.6 nm was observed. On cooling the sample, the *d* values increase again and reach a plateau region, followed by the transition to the gel phase. The hysteresis observed is consistent with the DSC results. To exclude the influence of the cooling rate on the spacings obtained from real-time X-ray diffraction measurements,[36,37] the cooling scan for **1a** has been stopped at 20.5 °C for 20 min while static exposures were taken. However, the diffraction data did not change during this time period.

The long spacings obtained on cooling compounds **1a** and **1b** are compared in Figure 9 (right). The general behavior of the *d* values in the gel and liquid-crystalline phases is qualitatively the same. For both substances, the L_α-phase can be supercooled with a remarkable increase of the *d* values. Both diastereomers show the plateau in the *d* values just before the main-transition as discussed above. The gel phases display the same bilayer thickness of about 5.6 nm. Compared to DPPC, which shows *d* spacings of about 6.0 nm, for compounds **1** smaller *d* spacings can be expected due to shorter acyl chains. In the experiment, a reduction in the *d* spacings of approximately 0.4 nm has been observed. Assuming an all-trans conformation of the chains, the length of the branched acyl chain decreases by about 0.38 nm (0.126 nm*3 CH_2-segments) compared to DPPC. Taking into account that the C16 ether residue at the C1 position of the glycerol remains constant, the asymmetric shortening of the acyl chain leads to a disturbance of the hydrophobic interactions. This could be compensated either by a stronger tilting of the chains and/or by a partial interdigitation of chains from adjacent bilayers. Therefore, the observed decrease in the gel phase spacings for **1a**/**b** compared with DPPC can be very well described by a partial interdigitation in the hydrophobic region keeping the tilt angle of the chains unchanged. Such chain packing leads to a slight distortion of the chain lattice indicated by the appearance of three reflections in the WAXS region.

At temperatures significantly above T_m, the temperature dependence of the *d* values is almost linear. However, when

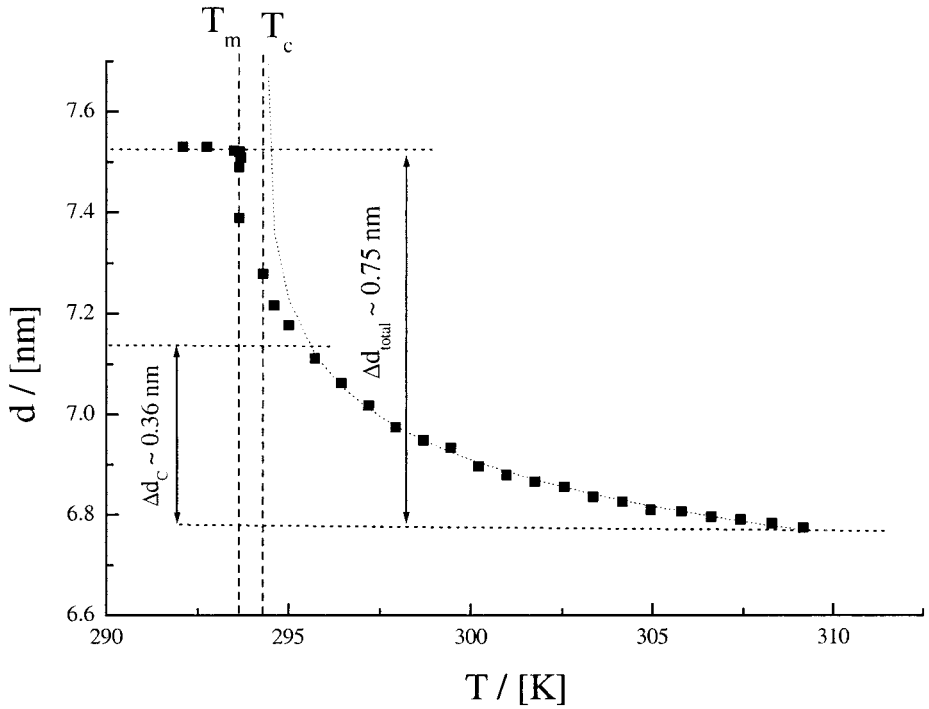

Figure 11. *d* spacings observed on cooling compound **1a** (■) and calculated *d* values (dotted line) as a function of temperature. T_C is the critical temperature used for the calculation of the *d* values and T_m is the main-transition temperature. The resulting critical swelling of the bilayer amounts to approximately 0.36 nm.

approaching the main-transition a strong nonlinear increase is observed. In previous investigations, this phenomenon has been described either in terms of analytical or critical behavior.[38] Assuming that we can describe the system in terms of a critical behavior, the temperature dependence of the *d* values is given by the following expression

$$d(T) \sim \left(\frac{T - T_C}{T_C}\right)^{-\alpha}$$

where T_C and α are the critical temperature and the critical exponent, respectively. The plot of $\ln(d) = f(\ln(|T - T_C/T_C|))$ should give a linear function that allows the determination of the critical exponent α. This relation is only valid for a certain T_C value. Therefore, varying T_C and fitting the linear expression allows the determination of the exact T_C value resulting from the plot of the correlation coefficient of the linear fit as a function of the critical temperature that has been used for the fit (Figure 10). Once T_C has been determined, the critical exponent can easily be calculated. Using this algorithm, a T_C value of 21.2 °C and a critical exponent of 0.021 46 have been obtained. Such an α value seems to be typical for lipid−water dispersions displaying a ripple phase between the liquid-crystalline L_α and the gel phase on cooling.[39] The experimentally determined *d* values and the calculated curve are shown in Figure 11. On cooling the sample, the *d* values follow the critical regime up to 22.5 °C (T_b). The magnitude of critical swelling of the bilayer amounts to approximately 0.35 nm. One reason for the critical swelling could be a change in headgroup hydration possibly connected with a change in the headgroup conformation. The resulting increasing area per lipid head could affect the local curvature of the membrane that can behave critically under certain conditions.[40] Between 22.5 and 21.2 °C (T_C), the *d* values increase by about 0.39 nm. However, in this temperature region the experimental data cannot be described by the expression deduced from critical behavior, suggesting that another driving force is responsible for the swelling. Therefore, the spacings above ~7.1 nm could be attributed to the start of chain ordering. Here we suggest that the critical swelling induces the modulation of the bilayer leading to the formation of a ripple phase $P_{\beta'}$. Therefore, the $P_{\beta'}$ phase observed in the X-ray diffraction patterns (Figure 7) can only appear in the cooling scans (monotropic phase transition). Compared to the nonbranched DMPC[39] compound **1a** exhibits a shorter acyl chain at the C2 position of the glycerol. Nevertheless, larger values for the critical and the noncritical swelling have been observed for **1a**. One reason for that could be the presence of the methyl branching close to the glycerol backbone, which disturbs the chain packing.

The present experiments show that the two pairs of diastereomers (*SS* + *RR* and *SR* + *RS*) isolated exhibit pronounced differences in the thermodynamically parameters of phase transitions both in two-dimensional (monolayers at the air/water interface) and three-dimensional systems (aqueous dispersions). However, the influence of the chiral carbon atoms is not strong enough to change the structure of the phases despite being able to affect their stability.

Acknowledgment. Financial support from the Deutsche Forschungsgemeinschaft (Emmy-Noether-Program grant BR 1826/2-1 and BR 1378/6-1) is gratefully acknowledged. The authors wish to thank Mrs. Barbara Elsner and Kristian Kjaer for excellent assistance.

References and Notes

(1) Small D. M. In *Handbook of lipid research, Vol. 4, The physical chemistry of Lipids*; Small D. M., Ed.; Plenum Press: New York, 1986; pp 475−522.
(2) Hatta I.; Kato S.; Takahashi H. *Phase Transitions* **1993**, *45*, 157.
(3) Lewis, R. N. A. H.; Mannock D. A.; McElhaney, R. N. In *Lipid Polymorphism and Membrane Properties*; Epand, R. M., Ed.; Academic Press: San Diego, 1997; pp 25−102.
(4) Lewis, R. N. A. H.; McElhany, R. N. *Biochemistry* **1985**, *24*, 2431.
(5) Menger, F. M.; Wood, M. G.; Zhou, Q. Z.; Hopkins, H. P.; Fumero, J. *J. Am. Chem. Soc.* **1988**, *110*, 6804.
(6) Nuhn, P.; Brezesinski, G.; Dobner, B.; Förster, G.; Gutheil, M.; Dörfler, H.-D. *Chem. Phys. Lipids* **1986**, *39*, 221.
(7) Nuhn, P. *Fett-Lipid* **1996**, *98*, 335.
(8) Brezesinski G.; Dietrich A.; Dobner B.; Möhwald H. *Prog. Colloid Polym. Sci.* **1995**, *98*, 255.
(9) Bringezu F.; Brezesinski G.; Nuhn P.; Möhwald H. *Biophys. J.* **1996**, *70*, 1789.
(10) Brezesinski, G.; Bringezu, F.; Weidemann, G.; Howes, P. B.; Kjaer, K.; Möhwald, H. *Thin Solid Films* **1998**, *329*, 256.
(11) Lewis, R. N. A. H.; McElhaney, R. N.; Harper, P. E.; Turner, D. C.; Gruner, S. M. *Biophys. J.* **1994**, *66*, 1088.
(12) Bringezu, F.; Brezesinski, G.; Möhwald, H. *Chem. Phys. Lipids* **1998**, *94*, 251.
(13) Rattay, B.; Brezesinski, G.; Dobner, B.; Förster, G.; Nuhn, P. *Chem. Phys. Lipids* **1995**, *75*, 81.
(14) Siegel, S.; Vollhardt, D.; Brezesinski, G.; Bringezu, F.; Möhwald, H. *Mat. Sci. Eng. C−Biomim. Supram. S* **1999**, *8−9*, 3.
(15) Zhang, R.; Sun, W.; Tristram Nagle, S.; Headrick, R. L.; Suter, R. M.; Nagle, J. F. *Phys. Rev. Lett.* **1995**, *74*, 2832.
(16) Chen, F. Y.; Hung, W. C.; Huang, H. W. *Phys. Rev. Lett.* **1997**, *79*, 4026.
(17) Lemmich, J.; Mortensen, K.; Ipsen, J. H.; Hoenger, T.; Bauer, R.; Mouritsen, O. G. *Phys. Rev. Lett.* **1995**, *75*, 3958.
(18) Helfrich, W. *J. Phys.* **1986**, *47*, 321.
(19) Lipowski, R. *Europhys. Lett.* **1988**, *7*, 255.
(20) Brezesinski, G.; Dietrich A.; Struth B.; Böhm C.; Bouwman W. G.; Kjaer K.; Möhwald H. *Chem. Phys. Lipids*, **1995**, *79*, 145.
(21) Bringezu F.; Dobner B.; Stritzel R.; Elsner B.; Nuhn P. *J. Chrom. A* **1996**, *724*, 367.
(22) Stritzel, R.; Dobner, B.; Bringezu, F.; Nuhn, P. *J. High Resol. Chrom.* **1996**, *19*, 121.
(23) Weitzel, G.; Wojahn, J. *Hoppe Seyler Zeitschr. f. Physiol. Chem.* **1950**, *285* 221.
(24) Stanley, W. M.; Joy, M. S.; Adams, R. *J. Am. Chem. Soc.* **1951**, *51*, 1261.
(25) Selinger, Z.; Lapidot, Y. *J. Lipid Res.* **1996**, *7*, 174.
(26) Lammers, J. G.; Liefkens, T. J.; Bus, J.; van der Meer, J.*Chem. Phys. Lip.* **1978**, *22*, 293.
(27) Dörfler, H.-D.; Brezesinski, G. *Colloid Polymer Sci.* **1983**, *261*, 286.
(28) Als-Nielsen, J.; Jaquemain, D.; Kjaer K.; Leveiller, F.; Lahav, M.; Leiserowitz, L. *Physics Rep.* **1994**, *246*, 251.
(29) Kjaer, K. *Physica B* **1994**, *198*, 100.
(30) Kaganer, V. M.; Möhwald H.; Dutta P. *Rev. Mod. Phys.* **1999**, *71*, 779.
(31) Rapp, G. *Acta Physica Polonica* **1992**, *A82*, 103.
(32) Rapp, G.; Gabriel, A.; Dosiere, M.; Koch, M. H. J. *Nucl. Instr. Methods A* **1994**, *291*, 178.
(33) Bringezu, F.; Brezesinski, G.; Nuhn, P.; Möhwald, H. *Thin Solid Films.* **1998**, *329*, 28−32.
(34) Weidemann, G.; Brezesinski, G.; Vollhardt, D.; Möhwald H. *Langmuir* **1998**, *14*, 6485
(35) Howes, P. B.; Kjaer K. *HASYLAB annual report*. **1996**, 445.
(36) Rappolt, M.; Rapp, G. *Ber. Bunsen-Ges. Phys. Chem.* **1996**, *100*, 1153.
(37) Cunningham, B. A.; Bras, W.; Lis, L. J.; Quinn, P. J. *J. Biochem. Biophys. Methods* **1994**, *29*, 87.
(38) Nagle, J. F. In *Phase Transitions in Complex Fluids*; Toledano, P., Neto, A. M. F., Eds.; World Scientific: Singapore, 1998.
(39) Richter, F.; Finegold L.; Rapp G. *Phys. Rev. E* **1999**, *59*, 3483.
(40) Taniguchi, T. *Phys. Rev. Lett.* **1996**, *76*, 4444.